PHOTOELASTIC INVESTIGATION OF STRESSES OF A SQUARE BEAM UNDER COMPRESSION

by

ALBERT CHANG-CHIH YEN
B. S., National Taiwan University, China, 1961

A MASTER'S REPORT

submitted in partial fulfillment of the
requirements of the degree

MASTER OF SCIENCE

Department of Applied Mechanics

KANSAS STATE UNIVERSITY
Manhattan, Kansas

1965

Approved by:

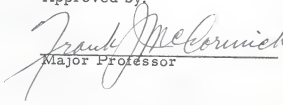

Major Professor

TABLE OF CONTENTS

INTRODUCTION

The problem of a square beam under axial compression is of both practical and theoretical interest. Professor J. M. Goodier in his paper entitled "Compression of Rectangular Blocks, and the Bending of Beams by Non-linear Distribution of Bending Forces" [3] has found an approximate stress function which satisfies the boundary conditions and the conditions of equilibrium but which does not necessarily give compatible strains, and from which stresses at points of a rectangular beam under compression can be calculated. In the discussion of that paper, Dr. Max M. Frocht suggested the possibility of solving this kind of problem by photoelastic methods. This is what was done for this report, i. e., an investigation was made of the stress distribution in a square beam which is under action of a pair of colinear forces. Although it is possible to find stresses at any point, the stress distributions along horizontal and vertical axes are of special interest, since these are the critical sections.

A BRIEF REVIEW OF THE THEORY OF TWO-DIMENSIONAL PHOTOELASTICITY

Certain Optical Fundamentals Used in Photoelasticity

The electromagnetic-wave theory, or simply the wave theory, is used to depict the behavior of light. Light is considered as a wave whose direction of vibration is perpendicular to its path and whose

amplitude can be expressed as

$$a = A \sin wt$$

where A is the maximum amplitude, and w is the circular frequency of radiation.

The velocity with which light propagates depends upon the material through which it passes. For certain material the velocity may further depend upon the plane in which light vibrates, i. e., light may propagate with different velocities in different planes. Each monochromatic light is specified by the frequency with which it vibrates and it is distinguished from the other through the sense of color. On the contrary, white light is made up of a number of constituent vibrations posessing different frequencies. When a certain color is spoken of, it is customary to refer to wave length (λ), instead of frequency (f), since the former is related to the latter by

$$c = \frac{\lambda}{f}$$

where c is the velocity of light in a vacuum.

Another convenient way to represent light is by a vector which has the magnitude of the amplitude and the direction of the vibration. This vector is called the light vector. Thus monochromatic light is represented by a single light vector, while white light is composition of a number of light vectors.

Light is said to be refracted when its velocity changes as it passes from one medium into another. The ratio of the velocities with which light travels in the two consecutive media is called the index of refraction.

One of the most important optical properties employed in the photoelastic method is polarization of light. Polarization means that the vibration of light is modified in a certain manner. Three kinds of polarization are very important to photoelasticity and are mentioned here:

Plane Polarization. Light is said to be plane-polarized when it is constrained to vibrate in only parallel planes, i. e., vibration is allowed in only one direction. In this case, the light vector has a constant direction, though its magnitude may change.

Circular Polarization. For circularly polarized light the light vector rotates around the line of propagation and has a constant magnitude. Circularly polarized light may be resolved into components in any two directions at right angles with the components having the same amplitude always.

Elliptical Polarization. This is essentially similar to circular polarization except that the magnitude of the light vector changes periodically during the rotation. Elliptical polarization is seldom used in photoelasticity.

Polarization of light is usually achieved by passing natural light or monochromatic light through a plate of crystal or a combination of crystal plates. The device used in this experiment to produce polarized light will be introduced later.

The Photoelastic Effect

Double Refraction or Birefrigence. Certain materials transmit only light vibrating in two selected perpendicular planes,

i. e., they polarize light in these planes and, in general, the velocity of transmission is not the same in the two planes. This phenomenon is referred to as "double refraction" or "birefringence." Materials used in photoelasticity must become birefringent when they are stressed.

Basic Optical Laws of Two-dimensional Photoelasticity. Almost all transparent materials such as glass, celluloid, Bakelite, and many other synthetic resins, become doubly refracting when they are subjected to stress. For normal incidence on flat plates subjected to plane stress within the elastic limit, there are two laws governing the relationships between the transmission of light and stress:

First, at any point in a stressed transparent plate, the axes of polarization of light passing through the solid are parallel to the direction of the principal stresses in the plane of the plate;

Secondly, the difference of the velocities of the two oppositely polarized rays at the point is proportional to the difference of these two principal stresses.

Thus by employing a suitable polariscope, information about the directions of the principal stresses and also the difference in their magnitudes can be obtained for any point. The directions of the principal stresses are shown by the isoclinic fringe patterns. The difference in the magnitudes of the principal stresses, which is twice the maximum shear, is given by the isochromatic fringe patterns. These are the basic data on which the stress analyses are to be made, with the help of the theory of elasticity.

INVESTIGATION OF A MODEL -- OBTAINING RAW TEST DATA

The Polariscope: The Chapman 8-inch research polariscope, of which a picture is given in Fig. 1, was used in this experiment. There is a dual lamp housing which contains a white light source and a monochromatic light source. The white light comes from a ribbon filament incandescent lamp, but the monochromatic light is obtained from a high intensity mercury vapor lamp equipped with glass filter passing the green light of 5461A^0 wave length.

All components and controls of this equipment are mounted on a single rigid steel tube that extends the length of the polariscope. The polarizer, the analyser, and the quarter-wave plates are all removable. Polariser and analyser can be coupled to rotate simultaneously. This last arrangement makes it possible to watch the movement of the isoclinic fringes.

Preparation of a Model: The first thing for preparation of a model is the selection of a material. Because of its ready availability, CR-39 was chosen for model material.

Some of the mechanical properties of CR-39 are given by Heywood [4] as: elastic limit = 3,000 psi, ultimate strength = 7,000 psi, and Young's modulus = 250,000 psi.

Although CR-39 is fairly sensitive to photoelastic effect, certain disadvantages it possesses may not be overlooked. That it creeps excessively is most undesirable and may often affect the quantitative accuracy of investigation. It also possesses a certain amount

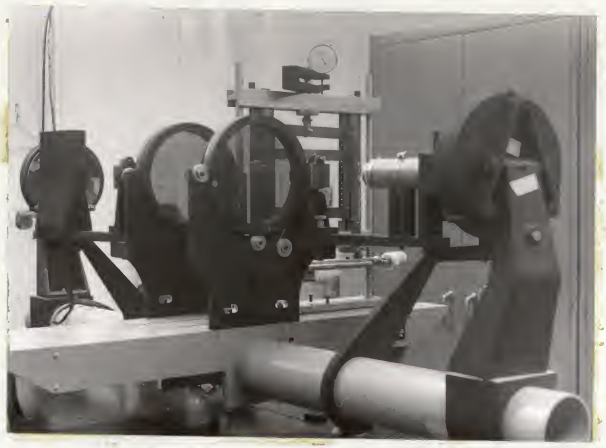

Fig. 1. The Chapman 8-inch research polariscope.

of initial stresses which sometimes prove to be troublesome. In spite of its very convenient form for the making of models, considerable care in machining is required to make a good model, for it is very prone to chipping; otherwise stresses may be developed on boundary by machining.

To make a model, the contour of the model was first outlined on a sheet of CR-39. For the purpose of this investigation, two models were to be made: One was a square beam of 1-1/2 inch sides for investigation, and the other was a 4.5 by 1.0 inch rectangular beam for use of calibration of the material. The Dremel Motor-Saw was used for rough cuts. The final rough cut would leave a margin around the desired contour about one-sixteenth inch wide. Then the model was secured to a suitable brass template having a desired contour with doubly-coated adhesive tape. The contour of the template used was rectangular. Finishing cut was made by a high-speed milling machine, which, in this experiment, is the Chapman Model Making Kit, Model 45. This final machine operation is illustrated in Fig. 2. The last step was to clean the finished models with trichloroethylene.

Loading Schemes. A pair of centered compressive forces were needed for the square beam. As approximation, uniformly distributed forces in width of one eighth of the depth of the beam were used instead. In Fig. 3, a sketch of loading jig for this compressive loading is given. It was difficult to get the two opposite forces exactly centered, and it should be noted that stresses obtained would vary according to the loading jig employed. In this experiment

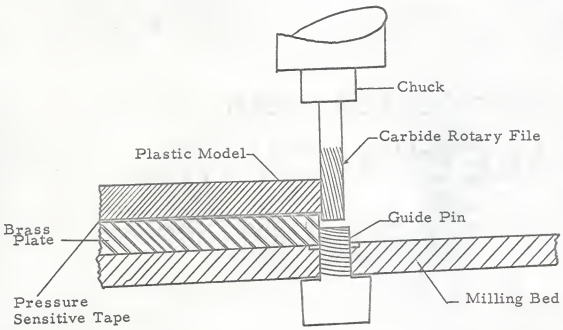

Fig. 2. Final machining of a photoelastic model.

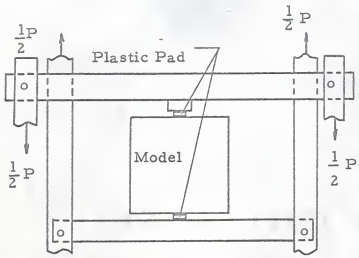

Fig. 3. Loading scheme for centered compression.

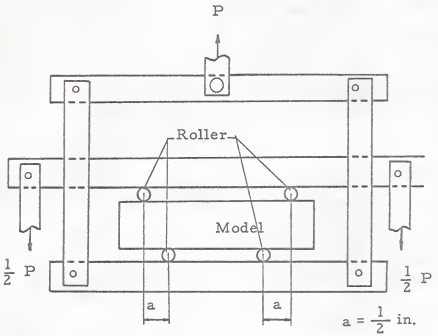

Fig. 4. Loading scheme for pure bending.

two plexiglass pads were used to transmit the load. If stresses of an actual beam are to be found by using a model, the loading jig used on the model must be exactly similar to that used on the actual beam.

For calibration, pure bending was used. The loading scheme is given in Fig. 4. Four brass rollers were used to transmit load.

Calibration for the Material. The pure bending method was used. From Strength of Materials the remotest fibre stress is given by the flexure formula

$$\tau_{max} = \frac{Mh}{2I}$$

where M is the applied moment, h is the depth of the beam, and I is the moment of inertia of the cross section about the neutral axis. But τ_{max} is also equal to C times N, where C is the stress-optical coefficient and N is the fringe order at top or bottom of the beam, i.e.,

$$\tau_{max} = \frac{Mh}{2I} = CN$$

from which

$$C = \frac{Mh}{2IN}$$

The dark field isochromatic photograph for the calibration (rectangular) beam under pure bending is shown in Fig. 5. To find N, a straight line was first obtained by plotting, for the middle section of the beam, fringe orders against distance from

Fig. 5. Dark field photograph of isochromatics for pure bending.

the horizontal center line, and is shown in Fig. 6. Then N was obtained by extrapolating the straight line to the boundary and found to be 5.55. The calculations for C are shown below

h = height of beam = 1.04"

b = thickness of beam = 0.267"

M = $\frac{1}{2}$ load times distance between right (left) adjacent rollers

$= \frac{1}{2}(30 \cdot 12.62) \cdot \frac{1}{2} = 94.5$ lb-in.

$N = 5.55$

$$C = \frac{Mh}{2IN} = \frac{12 \times 94.5 \times 1.04}{2 \times 0.267 \times 1.04^3 \times 5.55} = 370 \text{ psi/fringe}$$

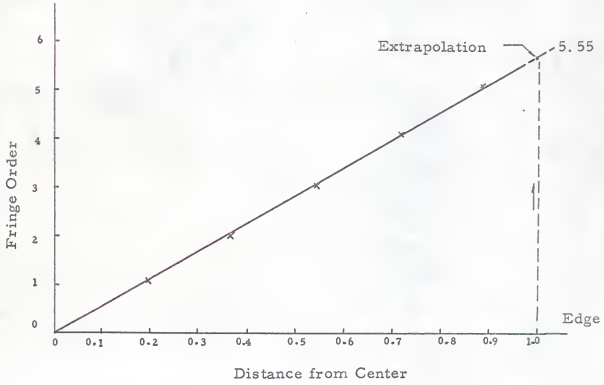

Fig. 6. Fringe order at edge by extrapolation.

Isochromatics. Circularly polarized monochromatic light was used to obtain the isochromatic fringe patterns. First, a dark field was obtained by crossed polarisers and crossed quarter-wave plates with the axes of the former make an angle of 45 degrees with those of the latter. Then a light field was obtained by rotating one of the quarter-wave plates to be parallel to the other.

After the arrangement for the proper polariscope being made, the model was loaded until enough isochromatic fringes were produced. The loading was allowed to stand for awhile until most creep occurred, and the fringe pattern did not change appreciably. Then the isochromatic photographs were taken, first for the dark field, and then for the light field. Kodak Contrast Process Panchromatic Films were used. The exposure time was one second. The photographs are shown in Fig. 7.

Isoclinics. Planely polarized white light was used for investigating the isoclinic fringe patterns. Although the directions of the principal stresses are independent of the magnitude of load, it was found that greater load might be practically necessary to bring out the isoclinics at regions where stresses were very small. Otherwise, either some of the isoclinics might be lost or appear fuzzy in those regions. Photographs were taken for the isoclinic patterns of parameters 5, 10, 15, 20, 25, 30, 35, 40, and 45 degrees.

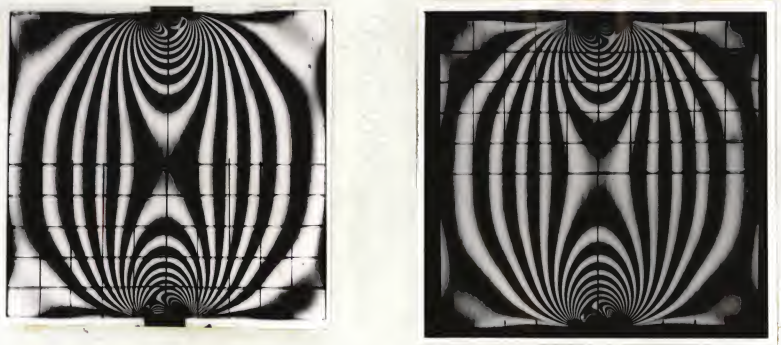

Fig. 7. Dark and light field photographs of isochromatics for the model.

These are enough to give complete information of direction of principal stresses when symmetry of the model and loading are taken into consideration. All photographs were taken with the film mentioned previously, but the exposure time was two seconds. The isoclinics of parameters 5 and 45 degrees are shown in Fig. 8.

With the aid of an enlarger, the isoclinics of different parameters were traced on one sheet of paper. This gave the complete isoclinic fringe pattern, one fourth of which is shown in Fig. 9, since the others can be obtained by reflecting it about the vertical and horizontal axes. Two isotropic points are presented in Fig. 9, which, together with others obtained from symmetry, make a total of six for the whole beam.

After the isoclinic fringe pattern was obtained, the stress trajectories (isostatics) were constructed by a graphical process on the basis of isoclinics [2]. Shown in Fig. 10 are the isostatics in one quarter of the beam. The p set represents the tensile stresses, while the q set represents the compressive stresses.

Fractional Fringe Order at Center. The directions of principal stresses at center, which are vertical and horizontal, are known from symmetry. Hence the Tardy method of compensation [3] was used to determine the fractional fringe order at that point. It was found to be 4.74 fringes. When P-Q curves along the vertical and horizontal axes of symmetry, where P and

(5^{o}) (45^{o})

Fig. 8. Photographs of 5^{o} and 45^{o} Isoclinics.

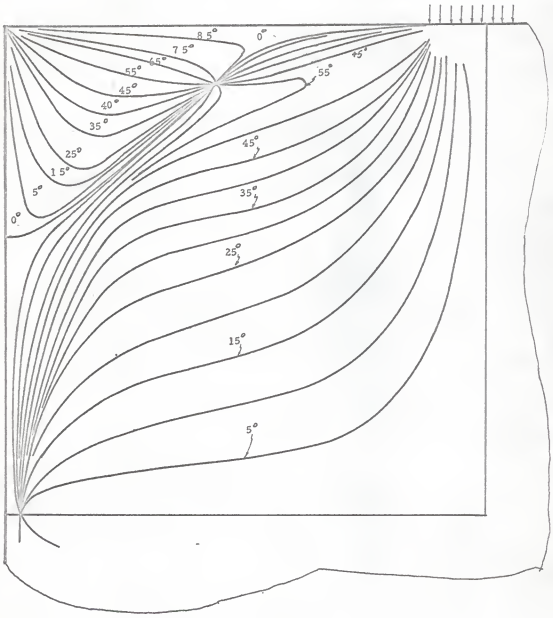

Fig. 9. Sketch of isoclinics.

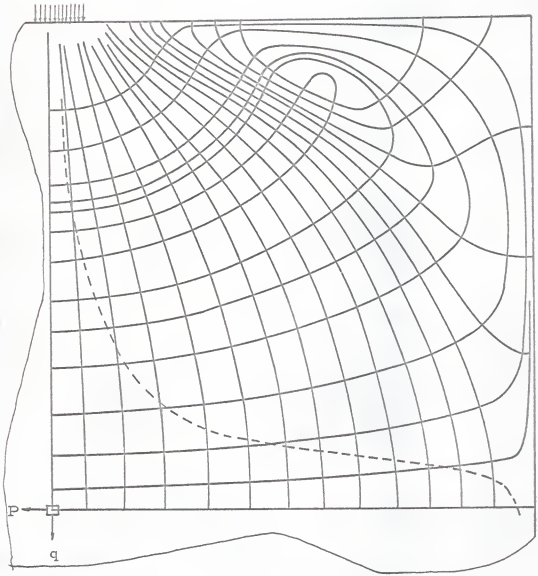

Fig. 10. Sketch of stress trajectories.

Q are principal stresses, were drawn, it was essential to know the fringe order at center.

SEPARATION OF STRESSES

Graphical integration of the Lamé-Maxwell equations and the shear difference method were employed to separate principal stresses. When symmetries of the model and loading were given full consideration, it was necessary to manipulate and analyze data for only one quarter of the square beam. For convenience of reference, that quarter was divided into a grid, as shown in Fig. 12. In the sequel two identical letters or numerals will stand for a section, and the intersecting point of a vertical and a horizontal section will be referred to by a letter and a numeral. The dimensions of the beam are given in Fig. 11. It is to be noted that the element of the grid in Fig. 12 is a square of side equal to one twentieth of the depth of the beam.

Stresses on the Axes of Symmetry. The Lamé-Maxwell equations were used to calculate the stresses on the axes of symmetry, AB and CD in Fig. 11, with the radius of curvature being computed graphically by using Fig. 10.

The stresses on the horizontal axis, namely, aa in Fig. 12, was first to be calculated. B, which is a_{10}, was chosen to be the starting point, since the P stress is zero there. In this case, one of the Lamé-Maxwell equations to be used was

$$\frac{\partial P}{\partial s_1} = \frac{Q - P}{\rho_2} \qquad (1)$$

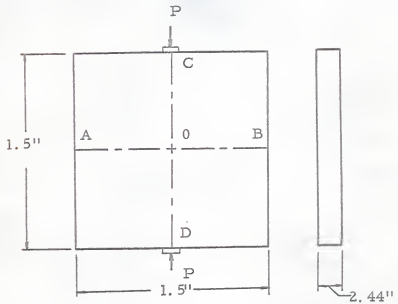

Fig. 11. Dimensions of the beam.

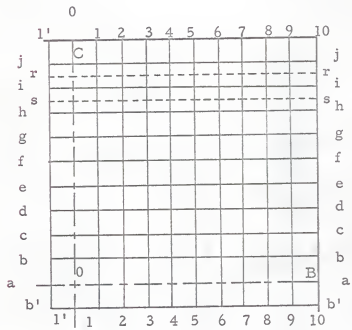

Fig. 12. Grid system used in stress analysing.

where s_1 is the distance measured along the p lines of principal stress in the direction BO, and ρ_2 is the radius of curvature of the intersecting q line.

As an approximation, ρ_2 can be written as

$$\rho_2 = \frac{\Delta s_2}{\Delta \phi}$$

where Δs_2 is a small displacement along the q line, and $\Delta \phi$ is the corresponding change in direction of the q line. Then (1) can be rewritten as

$$\frac{\partial P}{\partial s_1} = (Q - P) \frac{\Delta \phi}{\Delta s_2}$$

which, in increment form, is

$$\Delta P = (Q - P) \frac{\Delta s_1}{\Delta s_2} \Delta \phi \qquad (2)$$

By using (2) the increment ΔP can be calculated at points 9, 8, 7, ... and 0 on the section aa. Adding ΔP properly to P will give P for the above-said points successively.

In the actual calculation Δs_1 was taken as constant, being

$$\Delta s_1 = \frac{1}{20} \text{ depth of the beam.}$$

Δs_2 was taken as length of the q line between the 5 degree and the -5 degree isoclinics, which are the broken lines in Fig. 10. Hence $\Delta \phi$ was computed to be

$$\Delta \phi = -5^\circ - 5^\circ = -10^\circ = -0.175 \text{ radian}$$

The minus sign follows from the sign convention of the Lamé-

Maxwell Eq. [2]. The relations among $\Delta\phi$, s_1, and s_2 are illustrated by Fig. 13.

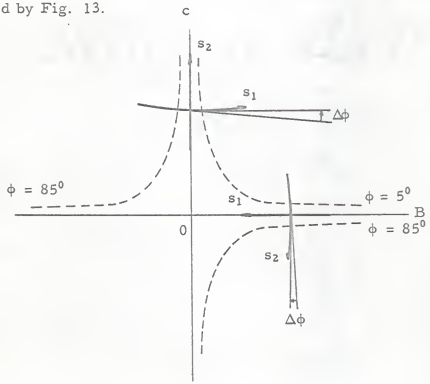

Fig. 13. Relation among ϕ, s_1, and s_2.

In Eq. (2) the ratio of Δs_1 to Δs_2 is needed. Thus they can be measured from Fig. 10 and their ratio can be computed immediately, instead of finding their lengths on the beam and their ratio.

The values of (Q-P) along aa are given in Fig. 14 in terms of fringes. The complete calculations are given in a tabulated form in Table 1.

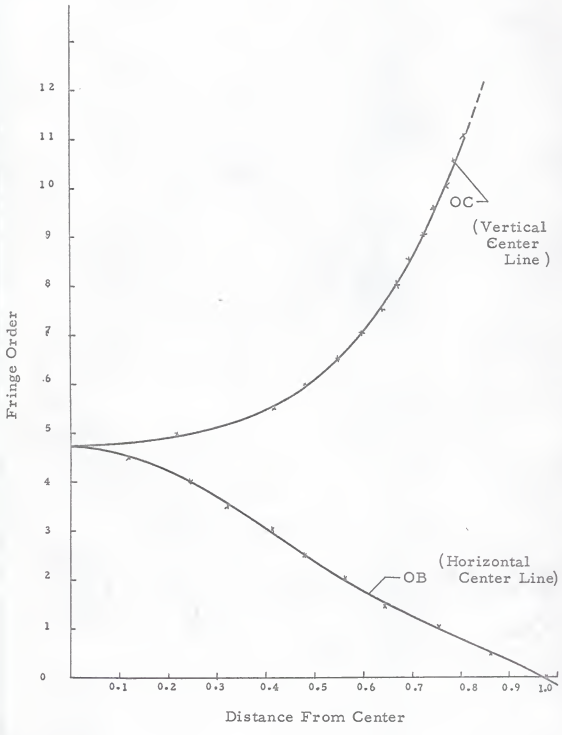

Fig. 14. Values of (P - Q).

Table 1. Calculations of principal stresses along horizontal symmetrical section.

$\Delta\phi$ = -0.175 rad Δs_1 = 25 unit (= 1 cm)

Station	Q-P fringes	Δs_2 unit	$\frac{\Delta s_1}{\Delta s_2} \cdot \Delta\phi$	ΔP fringes	ΔP (mean)	P fringes	Q fringes
10	+0.18	$-\infty$	0	0		0	+0.18
					0.022		
9	-0.32	+33	-0.133	0.043		0.022	-0.298
					0.060		
8	-0.76	+44	-0.0995	0.076		0.082	-0.678
					0.096		
7	-1.23	+47	-0.0932	0.115		0.178	-1.052
					0.125		
6	-1.78	58	-0.0755	0.134		0.303	-1.477
					0.151		
5	-2.47	64	-0.0685	0.169		0.454	-2.016
					0.172		
4	-3.05	72	-0.0609	0.176		0.626	-2.424
					0.186		
3	-3.7	83	-0.0528	0.195		0.812	-2.888
					0.174		
2	-4.22	122	-0.359	0.152		0.986	-3.234
					0.118		
1	-4.58	+240	-0.0182	0.084		1.104	-3.476
					0.042		
0	-4.74	$+\infty$	0	0		1.146	-3.594

By a similar procedure, stresses along section 00, which is OC in Fig. 11, can be found. The stresses of point O (a_0) have been found in Table 1. Therefore it is used as a starting point. Now the second equation of the Lamé-Maxwell equations is used. It is written as

$$\frac{\partial Q}{\partial s_2} = \frac{Q - P}{\rho_1}$$

where ρ_1 is the radius of curvature of p line. Like Eq. (2) it can be written in increment form

$$\Delta Q = (Q - P) \frac{\Delta s_1}{\Delta s_2} \Delta\phi \qquad (3)$$

Q can be found at points b_0, c_0, ... h_0 by using a similar argument to that employed previously. In this case Δs_2 is taken as constant, Δs_1 is the length of the p line between the 5 degree and the -5 degree isoclinics, and $\Delta\phi$ is 10 degrees. These relations are also shown in Fig. 13.

With the values of (Q-P) obtained from Fig. 14 and Δs_1 and Δs_2 measured from Fig. 10, ΔQ was computed from Eq. (3). Then Q was obtained after ΔQ was found. Calculations are tabulated in Table 2. It is to be noted that calculations cannot be carried beyond point h_0 since it is too near the load, and the photoelastic data is not reliable there.

Stresses on a Horizontal Section. The shear difference method may be used to separate stresses on a horizontal section. To give an illustration, section ii was worked

Table 2. Calculations of principal stresses along vertical symmetrical section.

$\Delta\phi$ = +0.175 $\qquad$ Δs_2 = 25 unit$(\frac{1}{2}'')$

	Q-P fringes	Δs_1 unit	$\frac{\Delta s_2}{\Delta s_1}\Delta\phi$	ΔQ fringes	ΔQ fringes	Q fringes	P fringes
0	-4.74	∞	0			-3.594	1.146
					-0.042		
b	-4.78	248	0.018	-0.084		-3.636	1.144
					-0.135		
c	-4.90	116	0.038	-0.185		-3.771	1.129
					-0.244		
d	-5.10	74	0.059	-0.301		-4.015	1.085
					-0.380		
e	-5.43	52	0.084	-0.457		-4.395	1.035
					-0.596		
f	-6.04	36	0.121	-0.734		-4.991	1.049
					-0.937		
g	-7.03	27	0.162	-1.140		-5.928	1.102
					-1.550		
h	-8.5	19	0.230	-1.960		-7.478	1.022
					-2.920		
i	-10.65	12	0.365	-3.890		-10.398	0.152

out only, and others can be obtained similarly. Cooridnate system and notations are shown in Fig. 15. The origin of coordinates coincides with i_{10} , x-axis with ii, and y-axis points down.

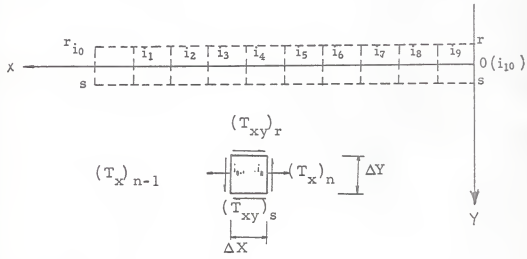

Fig. 15. Grid system for application of the shear difference method at section ii.

In a typical element shown in Fig. 15, T_x and T_{xy} are average stresses acting in the x-direction. Subscripts refer to faces they are acting on. Summing the forces in the x-direction yields an equation of equilibrium,

$$(T_x)_{n-1}\,\Delta Y - (T_x)_n\,\Delta Y - (T_{xy})_r\,\Delta X + (T_{xy})_s\,\Delta X = 0$$

which, rewritten, becomes

$$(T_x)_{n-1} = (T_x)_n - \left[(T_{xy})_r - (T_{xy})_s\right] \frac{\Delta X}{\Delta Y} \quad (4)$$

Since the value of T_{xy} can be computed at any point from isochromatic and isoclinic data by the formula

$$T_{xy} = \frac{P - Q}{2} \sin 2\phi ,$$

$(T_x)_{n-1}$ can be computed if $(T_x)_n$ is known and Δx and Δy are properly chosen. In this problem, Δx and Δy were chosen to be equal. $(T_{xy})_r$ was computed at $\frac{1}{2}(r_{n-1} + r_n)$ along section rr. So was $(T_{xy})_s$ along section ss. At i_{10} which is on the free boundary, the value of T_x is zero. So $(T_x)_n$, n = 9, 8, 7, ... 0, can be computed successively.

(P-Q) curves for sections rr, ii, and ss, which are obtained from Fig. 7, are given in Fig. 16. The values of ϕ, which is the angle between the x-axis and the p line, are obtained from Fig. 9, and given in Fig. 17.

The computations of T_x along ii are tabulated in Table 3. All stresses are expressed in terms of fringe order. The normal stress T_x along ii is plotted against distance in Fig. 18, which reveals its variation more clearly.

T_x at i_0 is obtained to be 0.24 fringes, which, at this special point, is also the principal stress P. Hence the other principal stress is

$$\begin{aligned} Q &= (Q - P) + P = (Q - P) + T_x \\ &= -10.65 + 0.24 \\ &= -10.41 \text{ fringes} \end{aligned}$$

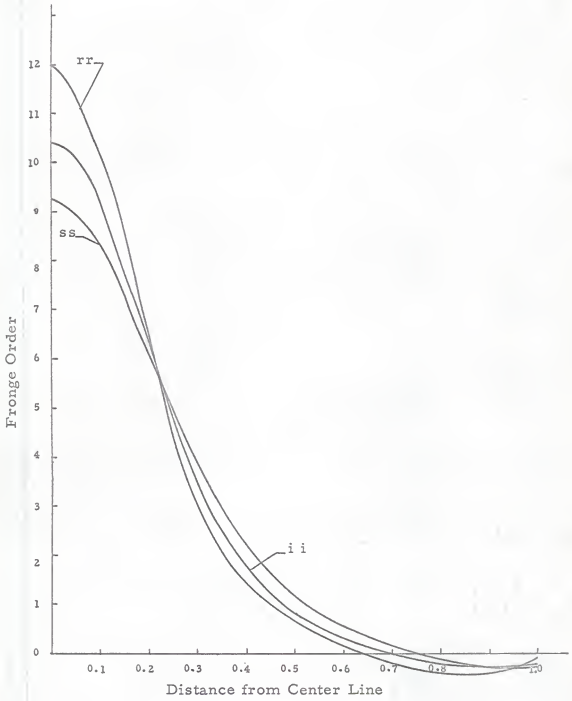

Fig. 16. Values of (P - Q).

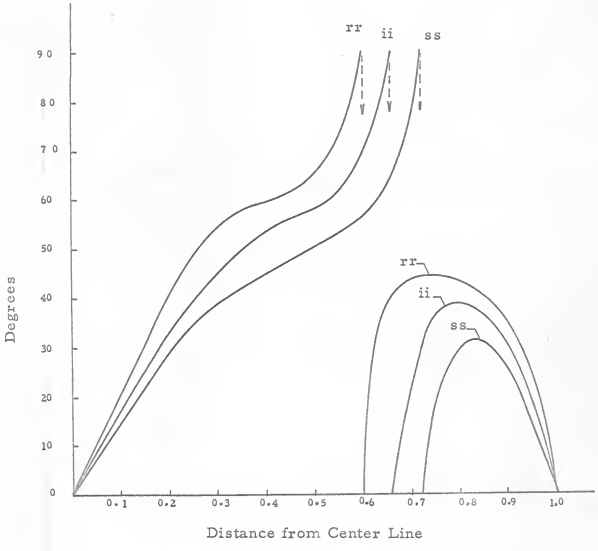

Fig. 17. Values of ϕ.

Table 3. Calculations of normal stress along section ii.

1	2	3	4	5	6	7	8	9
	Section rr			Section ss				
	$P\text{-}Q_{fringe}$	ϕ_{degree}	$(T_{xy})_r$	$P\text{-}Q_{fringe}$	ϕ_{fringe}	$(T_{xy})_s$	$(T_{xy})_r - (T_{xy})_s$	$(T_x)_n$
10								-0.0
9	-0.35	25.0	-0.14	-0.36	14.4	-0.07	-0.07	-0.07
8	-0.48	40.7	-0.24	-0.20	30.5	-0.09	-0.13	-0.20
7	-0.31	44.0	-0.154	+0.02	16.5	0.01	-0.14	-0.34
6	-0.01	39.0	-0.01	0.35	62.8	0.15	-0.16	-0.50
5	0.38	71.8	0.13	0.82	53.0	0.40	-0.27	-0.77
4	0.94	61.1	0.40	1.66	47.2	0.83	-0.43	-1.20
3	2.10	57.7	0.95	2.94	41.5	1.50	-0.55	-1.75
2	4.34	48.4	2.15	5.00	34.4	2.33	-0.18	-1.93
1	8.53	3.0	3.70	7.30	21.4	2.48	-1.22	-0.71
0	11.55	10.0	1.98	9.02	6.6	1.03	-0.95	+0.24

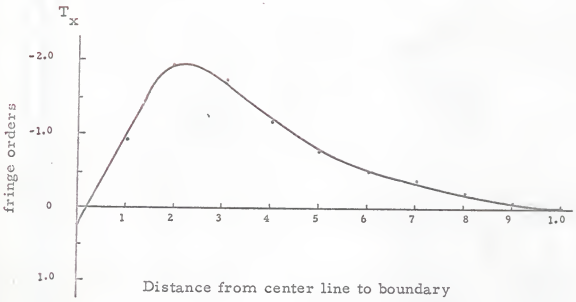

Fig. 17. Normal stress T_x along section ii.

These values compare with $Q = -10.398$ and $P = 0.252$ obtained previously and are very close.

For points other than i_o, the principal stresses Q and P can be deduced by use of the values of $(Q-P)$ and the relation

$$T_x = P \cos^2 \phi + Q \sin^2 \phi$$

Since this is not essential, it has not been carried through, but it can be done easily if desired.

DISCUSSION AND CONCLUSION

It is to be noted that the isochromatics, isoclinics, and the isostatics within the circular region of diameter equal to the depth of beam are closely similar to those of a circular disk under compression. It was difficult to determine these outside the circular region, since there are only relatively smaller stresses as well as stress differences. A glance at Fig. 9 reveals the congestion of isoclinics along the boundary of the circular region. As a matter of fact, when isoclinics were traced from the photographs of isoclinics of different parameters, sometimes it was almost impossible to distinguish one from the other. This may suggest an "isotropic ring" where principal stresses are equal or stresses are zero. But this is not the case. Careful study shows that there are only six isotropic points as were indicated previously. The two on the horizontal axis of symmetry are negative isotropic points and have non-interlocking isostatics in their neighborhood [2]. Others are positive isotropic points, where interlocking isostatics occur.

The accuracy of the graphic integration of the Lamé-Maxwell equations depends largely on the accuracy of the 5-degree isoclinics. A check has been afforded by finding the stresses at point i_0, using the shear difference method. In spite of the fact that the shear difference method may also introduce errors, the result of the check is reasonable. When further check is necessary, stresses on other

horizontal sections can be worked the same way.

Now a comparison will be made between the tensile stresses (T_x) along the vertical symmetric axis and those on a corresponding axis of a circular disk under compression. The latter stresses are constant, and referred to as T_0. The numerical value of T_0 will be computed for this experiment:

$$T_0 = \frac{2P}{\pi dt} = \frac{2 \times (20 \times 12.62)}{3.14 \times 1.5 \times 0.244} = 438 \text{ psi}$$

$$= \frac{438}{370} \text{ fringes} = 1.185 \text{ fringes}$$

where it is expressed in terms of fringe orders for convenience. Then the ratios T_x over T_0 can be calculated, using values of P in Table 2, and are shown in Table 4.

Table 4. Ratios T_x/T_0 along vertical axis.

Station	a	b	c	d	e	f	g	h	i
T_x/T_0	.966	.965	.954	.915	.874	.885	.928	.861	.213

It is to be seen that the maximum tensile stress of a square beam under compression occurs at center and is 0.966 of that of a circular disk. T_x/T_0 is also plotted against distance from center in Fig. 18. It is seen that T_x drops sharply after passing h, and will soon become compressive after passing i.

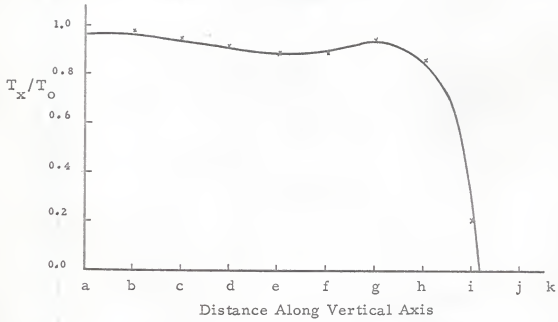

Fig. 18. T_x / T_0 along vertical axis.

The last thing to be mentioned is that by using the method developed by Professor Muskhelishvili in applying the theory of a complex variable to solve the plane stress problem, the problem of a square beam under compression can be solved exactly if an exact mapping function which maps the square into a unit circle can be found. Since this report stresses the application of the method of photoelasticity, the writer has not tried to solve this problem by the method just mentioned. Nevertheless, it would be interesting to try to do so, and might also be rewarding.

ACKNOWLEDGMENT

The writer wishes to express his sincere thanks to Professor F. J. McCormick for his guidance and suggestions in writing this report.

REFERENCES

1. Coker, E. G. and L. N. G. Filon. A Treatise on Photoelasticity. Cambridge University Press, 1957.

2. Frocht, M. M. Photoelasticity. Volumes I and II, New York: John Wiley and Sons, Inc., 1948.

3. Goodier, J. M. "Compression of Rectangular Blocks, and the Bending of Beams by Non-linear Distribution of Bending Forces." Trans. of ASME, Vol. 54, Apm 54-17, 1932.

4. Heywood, R. B. Design by Photoelasticity. London: Chapman and Hall, Ltd., 1952.

5. Jessop, H. J. and F. C. Harris. Photoelasticity. New York: Dover Publications, Inc., 1949.

PHOTOELASTIC INVESTIGATION OF STRESSES OF A SQUARE BEAM UNDER COMPRESSION

by

ALBERT CHANG-CHIH YEN

B. S., National Taiwan University, China, 1961

AN ABSTRACT OF A MASTER'S REPORT

submitted in partial fulfillment of the

requirements for the degree

MASTER OF SCIENCE

Department of Applied Mechanics

KANSAS STATE UNIVERSITY

Manhattan, Kansas

1965

Among the many techniques of experimental stress analysis the photoelastic method has been used more and more recently. In this investigation its advantage, particularly in the analysis of two-dimensional stress problems, is demonstrated through a practical application in solving a specific problem. The problem of a square beam under compression was chosen because of its theoretical and practical interest. This problem, simple as it may look, has presented difficulties in acquiring a theoretical solution. Only approximate solutions have been obtained. However, it is seen that, with relative ease, the problem was solved by the photoelastic method. In spite of the errors which may have been accumulated during the process of stress-separation, the results compare favorably with known mathematical solutions for the same problem.